Composite metamaterials with tunable chiral properties at terahertz frequencies

Jiaguang Han (韩家广)[1*], ZhenTian (田 震)[1], Jianqiang Gu (谷建强)[1], Mingxia He (何明霞)[1], and Weili Zhang (张伟力)[1,2]

[1] *Center for Terahertz Wave, Key Laboratory of Opto-electronic Information Science and Technology, Ministry of Education, College of Precision Instrument and Optoelectronics Engineering, Tianjin University, Tianjin 300072, China*

[2] *School of Electrical and Computer Engineering, Oklahoma State University, Stillwater, Oklahoma 74078, USA*

[*] *Corresponding author: jiaghan@gmail.com*

Received November 26, 2010; accepted January 19, 2011; posted online June 27, 2011

We propose a three-dimensional chiral metamaterial consisting of arrays of multi-layered mutually twisted sandwich metallic spirals. Such structure exhibits a negative refractive index at terahertz frequencies for its chirality. The chirality with varied refractive index can be achieved and tuned by changing the configurations. The presented structure offers flexibility for investigating electromagnetic properties of chiral metamaterials in the terahertz regime, thus leading to a unique route toward terahertz device applications.

OCIS codes: 350.3648, 160.3918, 300.6495.
doi: 10.3788/COL201109.S10401.

Metamaterial has attracted a great deal of attention owing to its significant experimental and theoretical interests, as well as its large potential applications. These intriguing applications have been involved in negative refraction[1−2], diffraction-limit breaking imaging[3−4], and cloaking[5−6]. In recent years, studies on metamaterials have been extended by introducing chirality conducted in metamaterials, named chiral metamaterials[7−13]. With endowed richer electromagnetic properties, chiral metamaterials not only support negative refraction generation, but also lead to many applications in photonic devices due to their strong polarization effect. The quest to achieve a three-dimensional chiral metamaterial with strong chirality and negative refractive index is in progress.

In this letter, we introduce a particular composite chiral metamaterial (CCM) at terahertz frequencies, which is the integration of sandwich structure and chiral metamaterial. The proposed structure is composed of multilayer sandwich metamaterials (metallic helixes), with each sandwich layer oriented against each other at a fixed angle. Due to the broken mirror symmetry, the building block is a three-dimensional structure of chiral characteristic. We theoretically demonstrate that the chiral properties of these CCMs are flexibly tunable in the terahertz regime by the change of orientation angle. The proposed CCM integrates the advantages of sandwich structure and helix design, and may lead to a possible way of achieving negative refraction and tunable chirality simultaneously.

The essence of designed CCM is based on a multilayer metallic helix sandwich resonator, in which the isotropic dielectric film with a thickness $d = 9$ μm is sandwiched by an alighted pair of metallic helixes to form one sandwich layer. Each layer is then cascaded to get a multi-layer design. Figure 1(a) shows the schematic of a unit cell of four-layer implemented CCM structure. In our simulations, the individual helix is made of a 200 nm-thick Aluminum film with a helix diameter of $R = 36$ μm and a linewidth of 4 μm. Each sandwich layer is spaced by a 50-μm thick dielectric spacer and then oriented by a fixed angle θ against each other to stack a multi-layer structure. The unit cell is then arranged in a square lattice with a lattice constant $P = 60$ μm, as shown in Fig. 1(b). The isotropic dielectric film and dielectric spacer in the simulations are chosen to be benzocyclobutene (BCB), a kind of polymer with 2.67 permittivity. All the dimensional parameters chosen here are typically used in the terahertz community in metamaterials research[14−16]. Computed simulations of the spectra response were performed using the commercial available finite-integration technique (FIT) software package (CST Microwave Studio).

In actual simulations, two normal incident orthogonal linear polarizations of light are employed to characterize the transmission of the sample polarization state[7,9], where transmission of the same polarization state is denoted as t_1 and that of perpendicular polarization state is as t_2. Figure 2(b) shows the calculated amplitudes of t_1 and t_2 for the CCMs with an orientation angle $\theta = 30°$. A strong resonance around 0.82 THz is visible as transmission minima, which is confirmed by the electric field

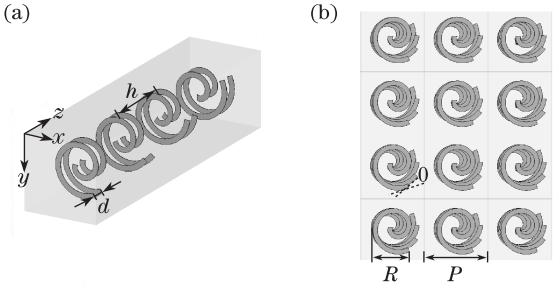

Fig. 1. (a) A unit cell of four-layer CCMs with $h = 50$ μm and $d = 9$ μm. The electromagnetic wave is incident along the z axis. (b) Schematic of a square array of CCMs of four layers with a period of $P = 50$ μm. The linewidth of metallic helix is 4 μm with a helix diameter of $R = 36$ μm. Each sandwich layer is oriented at a fixed angle θ.

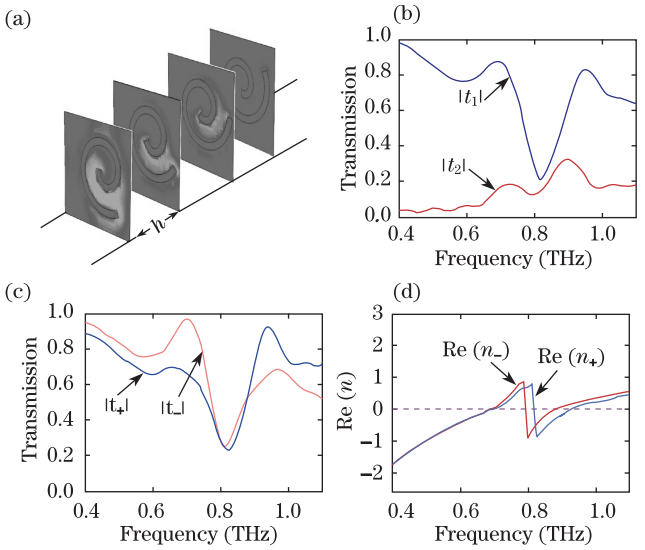

Fig. 2. (a) Electric field distribution of linear wave incidence at the resonance frequency of 0.82 THz. (b) Transmission amplitudes of t_1 and t_2. (c) Transmission amplitudes for RCP (t_+) and LCP (t_-) waves. (d) Retrieved real part of refractive index for RCP and LCP waves.

distribution shown in Fig. 2(a). The color field map in Fig. 2(a) depicts the evolution of the electric field for the linearly polarized wave propagation through each layer at the resonance frequency. For the incident linear polarized wave, the electric field is strongly localized around the arms of the metallic helix, and then significantly twisted and perturbed by different layers.

Using the obtained t_1 and t_2, we translate them into the transmission for right circular polarization (RCP), t_+, and, left circular polarization (LCP), t_-, of the incident light by[7,9], $t_+ = t_1 + i\,t_2$ and $t_- = t_1 - i\,t_2$. Figure 2(c) shows the transmissions for both circularly polarized beams. The resonance for both RCP and LCP is around 0.82 THz, but the difference between them is remarkable, indicating chiral properties. The physical origin of the chirality of the studied CCMs lies in the fact that the oriented helix sandwich layers break the mirror symmetry. Electromagnetic response of the chiral feature can be described by the relationship between electric flux density D, magnetic flux density B, electric field strength E, and magnetic field strength H

$$\begin{pmatrix} D \\ B \end{pmatrix} = \begin{pmatrix} \varepsilon_0\varepsilon & i\xi/c_0 \\ -i\xi/c_0 & \mu_0\mu \end{pmatrix} \begin{pmatrix} E \\ H \end{pmatrix}, \qquad (1)$$

where ε_0, μ_0, and c_0 are the permittivity, permeability, and speed of light in vacuum, respectively; ε, μ, and ξ are the effective permittivity, effective permeability, and chiral parameter of the metamaterials. Refractive index of the chiral media for RCP and LCP is given by: $n_\pm = \sqrt{\varepsilon\mu} \pm \xi$. The relationship clearly shows that if one metamaterial shows chirality, the refractive index would be highly related with its chiral properties. Figure 2(d) shows the real part of refractive index for both LCP and RCP waves, in which the retrieval of effective parameters of the studied structure is based on the calculated complex coefficients of both transmission and reflection. Around the resonance at 0.82 THz, the real part of the refractive index of LCP shows negative value between 0.79 and 0.87 THz, while that of RCP is less than zero between 0.82 and 0.92 THz. At a frequency ranging from 0.82 to 0.87 THz, the real parts of the refractive index for both circular waves reach negative values. The negative refraction below 0.7 THz is ascribed to the other resonance of the CCM at lower frequency, where the resonance is similar to that induced in the normal sandwich structure without chirality.

With regard to the negative refraction that occurred in sandwich metamaterials, previous reports have presented detailed discussions[14]. Briefly, if the electric resonance induced by the pair of metallic structure of the sandwich metamaterial is overlapped with the magnetic resonance induced by its opposing metallic structures within one elementary cell, a left-handed behavior of negative refractive index can thus be observed. In this case, the negative refraction is primarily due to the simultaneous negative permittivity and permeability. In our designed CCMs, the lower resonance occurring around 0.21 THz belongs to this case. Moreover, we notice that optical spectra of this case are almost independent from the polarizations of incident circular waves. From this viewpoint, we can see that negative refraction exists in the CCMs because of not only superimposed electric and magnetic resonances, but also the chirality, especially the CCM at 0.82 THz, whose negative refraction is highly connected with the latter.

To better understand the behaviors of the proposed CCMs, we show the calculated amplitudes of t_+ and t_- as a function of rotation angle θ ranging from 0 to 90°. As shown in Fig. 3, with the increase of θ from 15 to 60°, the difference between amplitudes of t_+ and t_- are enhanced, while further increase of θ to 90° makes the difference smaller. When $\theta = 90°$, the transmission for both RCP and LCP is almost consistent with each other due to the disappearance of chirality resulting from the rotation symmetry of the CCM structure. Figure 3(b) shows the obtained real part of refractive index for various θ. When $\theta = 15°$, the real part of refractive index for RCP is positive while that for LCP is almost negative. When θ increases to 75°, the real part of refractive index for RCP becomes completely positive at the resonance around 0.8 THz, but that for LCP still shows negative value. When θ is 90°, the chirality almost disappears and the real part of

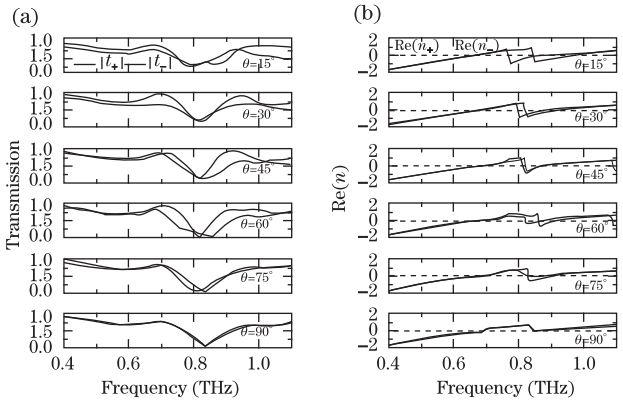

Fig. 3. (a) Transmission amplitude for RCP and LCP waves as a function of orientation angle θ. (b) Retrieved real part of refractive index for RCP and LCP waves at various θ.

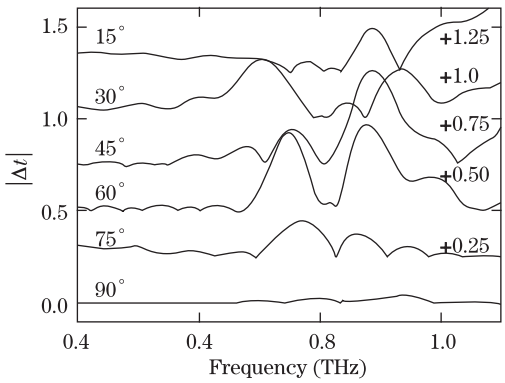

Fig. 4. Differences between the transmission of RCP and LCP waves at different orientation angle θ. The offset is 0.25.

index for RCP becomes quite the same as that for LCP and shows a positive value. Hence, the negative index feature of CCMs around 0.8 THz is clearly highly related to its chiral properties.

The differences in transmission are also characterized by $|\Delta t| = |\,|t_+| - |t_-|\,|$. In Fig. 4, $|\Delta t|$ as a function of θ is presented. Obviously, $|\Delta t|$ is enhanced initially and then reduced with increasing θ. This tunable behavior provides flexibility for one to design metamaterials when considering chiral properties and negative index features.

In conclusion, we have proposed a design for negatively refracting chiral metamaterials in the terahertz regime based on arrays of multi-layered mutually twisted sandwich metallic spirals. For terahertz wave propagation through the structure, optical responses for the two circularly polarized waves show the remarkable differences around the resonance frequency. The achieved strong chirality thus allows for the realization of negative refraction. Chirality and refractive index are highly related to the designed configurations, where a tunable chiral property can be achieved by changing the twisted angles. The proposed designed is scalable to other frequency regions and can be used in optically active terahertz devices.

This work was partly supported by the National Natural Science Foundation of China (No. 61007034) and the National Key Basic Research Special Foundation of China (No. 2007CB310403).

References

1. R. A. Shelby, D. R. Smith, and S. Schultz, Science **292,** 77 (2001).
2. Z. Liu, H. Lee, Y. Xiong, C. Sun, and X. Zhang, Science **315,** 1686 (2007).
3. K. Kawase, Y. Ogawa, Y. Watanabe, and H. Inoue, Opt. Express **11,** 2549 (2003).
4. I. I. Smolyaninov, Y.-J. Hung, and C. C. Davis, Science **315,** 1699 (2007).
5. J. B. Pendry, D. Schurig, and D. R. Smith, **312,** 1780 (2006).
6. D. Schurig, J. J. Mock, B. J. Justice, S. A. Cummer, J. B. Pendry, A. F. Starr, and D. R. Smith, Science **314,** 977 (2006).
7. S. Zhang, Y.-S Park, J. Li, X. Lu, W. Zhang, and X. Zhang, Phys. Rev. Lett. **102,** 023901-1 (2009).
8. J. K. Gasnsel, M. Thiel, M. S. Rill, M. Decker, K. Bade, V. Saile, G. von Freymann, S. Linden, and M. Wegener, Science **325,** 1513 (2009).
9. E. Plum, J. Zhou, J. Dong, V. A. Fedotov, T. Koschny, C. M. Soukoulis, and N. I. Zheludv, Phys. Rev. B **79,** 035407-1 (2009).
10. M. Decker, M. W. Klein, M. Wegener, and S. Linden, Opt. Lett. **32,** 856 (2007).
11. A. Demetriadou and J. B. Pendry, J. Phys.: Condens. Matter **21,** 376003 (2009).
12. T. G. Mackay and A. Lakhtakia, SPIE Reviews **1,** 018003-1 (2010).
13. B. Wang, J. Zhou, T. Koschny, M. Kafesaki, and C. M. Soukoulis, J. Opt. A: Pure Appl. Opt. **11,** 114003 (2009).
14. J. Gu, J. Han, X. Lu, R. Singh, Z. Tian, Q. Xing, and W. Zhang, Opt. Express **17,** 20307 (2009).
15. J. Gu, Z. Tian, Q. Xing, C. Wang, Y. Li, F. Liu, L. Chai, and C. Wang, Chin. Opt. Lett. **8,** 1057 (2010).
16. Y. Wang, Z. Zhao, Z. Chen, L. Zhang, and K. Kang, Chin. Opt. Lett. **7,** 690 (2009).